12WCEE 2000

0073

PERFORMANCE COMPARISON OF DIFFERENT FRICTION DAMPED SYSTEMS

Yaomin FU[1] And Sheldon CHERRY[2]

SUMMARY

In this paper, proportional friction damped (PFD) systems are modelled according to their hysteretic properties. A "resolution-synthesis" approach is applied to PFD systems to derive closed-form solutions for system spectral response estimates. These solutions, and similar previously developed solutions for constant friction damped (CFD) systems, are verified by comparing the values obtained from the closed-form solutions with the corresponding results derived from a series of dynamic time history response analyses. The closed-form solutions are then used to examine the influence of the basic system parameters on system response in order to provide a guide for optimal design. The abilities of the PFD and CFD systems in reducing seismic response are compared on the basis of their response estimates for a given primary system.

INTRODUCTION

Various types of friction dampers are used to mitigate seismic hazards in structural systems. The effectiveness of a friction damper in reducing seismic response depends on its hysteresis property, which in turn is characterized by the damper slip force. Friction dampers whose slip forces are constant (CFD) produce hysteretic loops that are essentially rectangular in shape, whereas dampers whose slip forces are proportional to the damper displacement (PFD) produce hysteresis loops that have a flag-shape or triangular-shape appearance.

The damper slip force is determined by the normal force acting on the friction surface in the damper. In a CFD, a constant slip force is developed by applying a constant normal force to the slip surfaces. This constant normal force can be assured by using either pre-stressed bolt mechanisms [Pall and Marsh 1982; Filiatrault and Cherry 1987; Tremblay and Stiemer 1993; Grigorian and Popov 1993] or pre-stressed longitudinal spiral spring-wedge mechanisms [Aiken and Kelly 1990]. In a PFD, the displacement-proportional slip force is produced by a displacement-proportional normal force. This proportional normal force can be achieved by using either a longitudinal spiral spring-wedge mechanism [Nims et al 1993], or a ring spring-wedge mechanism [Shepherd and Erasmus 1988; Kar et al 1996]. In general, the PFDs possess a self-centering feature, while the CFDs can dissipate more energy per cycle than the PFDs for a given slip force and displacement amplitude. Both types of friction dampers can be used to control the seismic response of structures.

In this paper, a recently developed "resolution-synthesis" approach is employed to establish the closed-form solution for a PFD system, from which an estimate of the system spectral response can be obtained; the corresponding solution for a CFD system is available in the authors' previous studies [Fu and Cherry 1999c]. This approach has been successfully applied to velocity-dependent passive energy dissipation systems (Fu 1996; Fu and Kasai 1998), bilinear displacement-dependent passive energy dissipation systems [Watanabe 1996; Kasai et al 1998], and trilinear displacement-dependent passive energy dissipation systems [Fu and Cherry 1998, 1999a, 1999b, 1999c]. In the approach, the spectral response of a friction damped system is normalized with respect to the response of a linear system, and then resolved into individual terms that take into account the

[1] *Visiting Researcher, Dept. of Civil Engineering, U of British Columbia, Vancouver, BC V6T 1Z4, Canada*
[2] *Professor Emeritus, Dept. of Civil Engineering, U of British Columbia, (phone) 604-822-2602,(e-mail) cherry@civil.ubc.ca*

separate response effects caused by the period shift and damping increase associated with the damped system. The combination of these individual terms, for which credible expressions are available, produces a closed form solution for the friction damped system response, which depicts the system performance in terms of its controlling parameters. The normalized response functions obtained for the PFD and CFD systems are verified by the results obtained from a series of dynamic analyses. The influence of changes in the system parameters on system performance are then clearly illustrated through a parametric study, which provides the range of system parameters that lead to an optimal design. This approach is more informative and efficient than performing a series of dynamic analyses to obtain information that is capable of defining the optimal design of a friction damped system. Finally, the seismic performance of single degree of freedom (SDOF) systems equipped with CFD and PFD are compared for situations when their parametric conditions are identical.

CLOSED FORM SOLUTION FOR PFD SDOF SYSTEMS

Model of PFD systems

A proportional friction damper (PFD) can be modelled by a spring and a friction mechanism that are connected in parallel, as shown in Fig. 1a. The spring has a stiffness, K_d. The normal force in the friction mechanism is proportional to the spring force. Thus, the slip force of the friction mechanism is proportional to the spring force, or mechanism displacement. The damper may have an initial displacement Δ. The resisting force provided by a PFD can be expressed as:

$$f = \begin{cases} (1+\eta')K_d(u+\Delta) = K_d'(u+\Delta) & \textit{when loading} \\ (1-\eta'')K_d(u+\Delta) = K_d''(u+\Delta) & \textit{when unloading} \end{cases} \quad (1)$$

where u is the system displacement relative to its base, η' and η'' are the ratios of the slip force to the spring force for the loading and unloading condition, respectively. As shown in Fig. 1a, the hysteresis loop of a PFD can have triangular-shape (T-PFD) when Δ=0, or a flag-shape (F-PFD) when Δ>0. Note that the hysteresis loop is symmetric with respect to the origin. The loop corresponding to the negative displacement is omitted in Fig. 1 to save space.

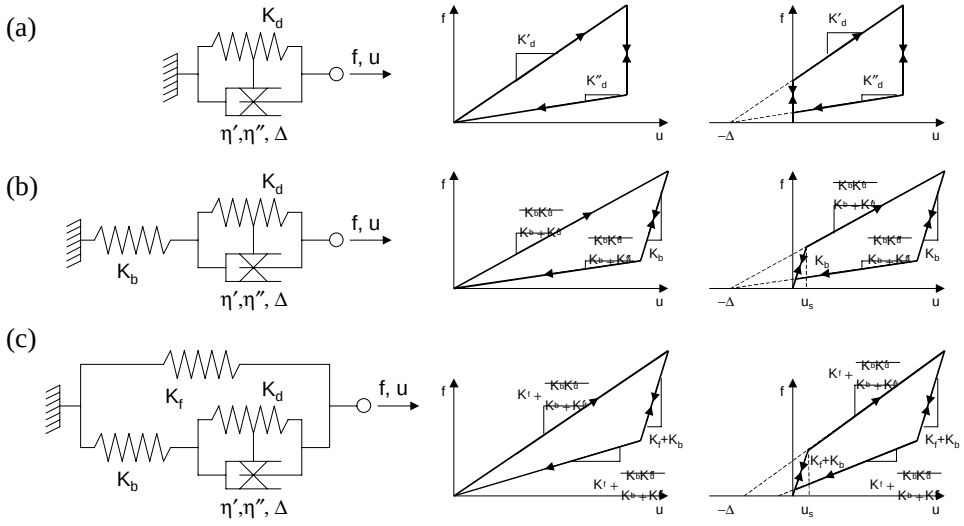

Figure 1. Model and hysteresis loops of PFD system: (a) PFD damper; (b) PFD unit; (c) PFD SDOF system

Fig. 1b shows a PFD damper connected in series with a bracing member to form a PFD unit model. The bracing stiffness, K_b, significantly influences the effectiveness of a PFD on seismic response reduction [Nims et al 1993]. It may be seen that the displacement of the hysteresis loop of a PFD unit is increased as a result of the bracing.

Fig. 1c depicts the model of the PFD SDOF system studied in this paper. For seismic response analysis, the system mass, M, is located at the right node and the system base is excited by a selected ground motion. In the

present study, it is assumed that the frame is protected from yielding. The frame stiffness is K_f. The total system resisting force is the summation of the PFD unit force and the frame force. The arrows on the hysteresis loops in Fig. 1 describe the loading and unloading paths. In a F-PFD system, the damper slippage starts at the slip displacement u_s and ends at a displacement smaller than u_s. A T-PFD system behaves pseudo-elastically; its hysteresis characteristic does not change with respect to displacement.

Equivalent linearization of PFD system

To apply the "resolution-synthesis" approach to a PFD system, it is first necessary to replace it by an equivalent linear system. This system, which is represented by an equivalent period and damping ratio, is used to approximate the maximum seismic displacement of the PFD system. Among various linearization techniques, the average stiffness and energy (ASE) method proposed by Iwan and Gates [1979] is considered to be versatile and is adopted by the authors in this study. According to the ASE method, the equivalent stiffness K_e and the dissipated energy E_{de} are calculated from the following integrals [Iwan and Gate 1979; Fu and Cherry 1999c]:

$$K_e = \frac{1}{u_{\max}} \int_0^{u_{\max}} K_{\sec}(A)dA = K_f K_{eo}\,, \quad E_{de} = \frac{1}{u_{\max}} \int_0^{u_{\max}} E_d(A)dA = 2K_f u_{\max}^2 E_{do} \tag{2a}$$

For F-PFD systems:

$$K_{eo} = 1 + \frac{\alpha_b(\alpha_b + \alpha_b \ln \mu_s + \alpha_d'\mu_s}{\mu_s(\alpha_b + \alpha_d')}\,,\ E_{do} = \frac{\alpha_b^2 \alpha_d'(1 - K_d''/K_d')}{6(\alpha_b + \alpha_d')^2} \frac{(\mu_s - 1)^2}{\mu_s^3}(\mu_s + 3\frac{\alpha_b}{\alpha_d'} + 2) \tag{2b}$$

For T-PFD systems:

$$K_{eo} = 1 + \frac{\alpha_b \alpha_d'}{\alpha_b + \alpha_d'}\,, \qquad E_{do} = \frac{\alpha_b^2 \alpha_d'(1 - K_d''/K_d')}{6(\alpha_b \alpha_d')^2} \tag{2c}$$

where:

$$\alpha_b = \frac{K_b}{K_f}, \quad \alpha_d' = \frac{K_d'}{K_f}, \quad \mu_s = \frac{u_{\max}}{u_s} = \frac{K_b}{K_d'}\frac{u_{\max}}{\Delta} \geq 1 \tag{2d}$$

In Eqs. 2a to 2d, $K_{sec}(A)$ is the secant stiffness at any displacement A on the skeleton curve of the PFD system; in the ASE method, by definition, the skeleton curve is the loading path of the hysteresis loops shown in Fig. 1. $E_d(A)$, which is the energy dissipated per cycle, is equal to the area contained within the hysteresis loops when the displacement is A. α_b is the brace stiffness ratio, α_d' is damper stiffness ratio, and μ_s is damper slip ratio.

Since the period of a linear system is proportional to the square root of its stiffness, and its equivalent viscous damping ratio can be evaluated by dividing the energy dissipated per cycle by 4π times the strain energy, the period, T_e, and damping ratio, ξ_e, of the equivalent linear system can be established using the preceding results:

$$T_e = \sqrt{\frac{K_f}{K_e}} T_f = \sqrt{\frac{1}{K_{eo}}} T_f\,, \quad \xi_e = \xi_o + \frac{E_{de}}{2\pi K_e u_{\max}^2} = \xi_o + \frac{E_{do}}{\pi K_{eo}} \tag{3}$$

where $T_f = 2\pi(M/K_f)^{1/2}$ and ξ_o are, respectively, the period and the inherent damping ratio of the primary linear system consisting of its spring stiffness K_f and mass M. Note that the fundamental parameters for determining the behaviour of the PFD system are α_b, α_d', μ_s, K_d''/K_d', T_f and ξ_o.

Normalized displacement function

By definition (Fu and Cherry 1999c), the normalized spectral displacement of a linear passive energy dissipation system is:

$$R_{sd} = \frac{S_d(T_e,\xi_e)}{S_d(T_f,\xi_o)} = \left[\frac{S_d(T_e,\xi_e)}{S_d(T_e,\xi_o)}\right]\left[\frac{S_d(T_e,\xi_o)}{S_d(T_f,\xi_o)}\right] = \left[\sqrt{\frac{(1-e^{-B\xi_e})\xi_o}{(1-e^{-B\xi_o})\xi_e}}\right]\left[\sqrt{\frac{1}{K_{eo}}}\right] \tag{4}$$

where $S_d(T_e, \xi_e)$ and $S_d(T_f, \xi_o)$ represent the spectral displacements of a damped system and its primary system, respectively. R_{sd} reflects the change in spectral displacement due to the insertion of the damper into a primary system. The two bracketed terms in Eq. 4 separate this change into two parts. The first part reflects the response reduction caused by damping change. The reduction rule proposed by Hanson and Jeong [1994], where B=30, is adopted to evaluate the displacement reduction due to damping. The second part reflects the displacement change caused by the equivalent period shift. This change is calculated from the smooth spectrum shape. It is assumed that the system period falls within the constant velocity region of the spectrum. Thus, the displacement change due to period shift is proportional to the period change, which, by involving Eq. 3, leads to the above expression.

Note that the normalized functions of systems with different dampers are derived from expressions that are identical to Eqs. 2a, 3 and 4, but whose individual parameters given by Eqs. 2b, 2c and 2d differ. For a bilinear constant friction damped (CFD) system whose schematic model and hysteresis loop are shown in Fig. 2, the equations corresponding to Eqs. 2b, 2c, and 2d are [Fu and Cherry 1999c]:

$$K_{eo} = 1 + \alpha_b \frac{1+\ln\mu_s}{\mu_s}, \quad E_{do} = \alpha_b \frac{(\mu_s - 1)^2}{\mu_s^3} \tag{5a}$$

$$\alpha_b = \frac{K_b}{K_f}, \quad \mu_s = \frac{u_{\max}}{u_s} = \frac{K_b u_{\max}}{P_s} \geq 1 \tag{5b}$$

where P_s is the damper slip force.

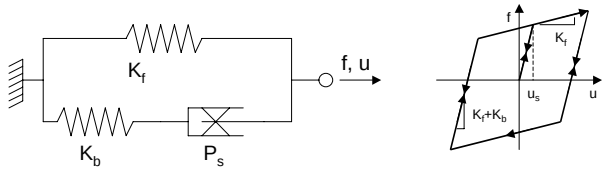

Figure 2 Model and hysteresis loop of bilinear CFD system

DYNAMIC VERIFICATION

The closed-form solutions obtained for the normalized displacement of the F-PFD, T-PFD and CFD systems were verified by comparing their values, determined for various system parameters, with the ratios of the spectral displacements of the damped and the primary systems corresponding to these same parameters. These latter spectral displacements were calculated by employing dynamic response analyses. The primary system used in the verification study has a period T_f =2.5 second and an inherent damping ratio ξ_o=0.02; these values were not varied in this study. The values assigned to the system parameters in this verification study were: α_b=2 and 10, α_d'=0.1 for F-PFD system and 0.1 to 2.5 for T-PFD system, μ_s=1 to 40, K_d''/K_d'=0.1. These ratios represent reasonable, practical values and correspond to ranges for which the significance of using friction dampers is later shown to be apparent. Ten natural earthquake records were used in the dynamic analyses; they are: El Centro (1940 NS), Taft (1952 EW), Hachinohe (1968 EW), Parkfield (1966 CSA2 N65E), Mexico (1985 SCT EW), Sylmar (1994 Northridge CHPL NS), Pacoima (1971 San Fernando N164E), Newhall (1994 Northridge LA CFS NS), Olympia (1965 N266E), and Loma Prieta (1989 Gilroy 2SHCB NS). The 2% damping spectra of these records, normalized to a one meter displacement at period 2.5 second, are shown in Fig. 3. It can be seen that in the expected period shift range (1.3 sec. to 2.5 sec.) the average velocity spectrum is reasonably constant and the average displacement spectrum tends to straight line, thereby suggesting the assumption associated with Eq. 4 is satisfied. The RUAUMOKO software program was used for the dynamic analyses [Carr 1998].

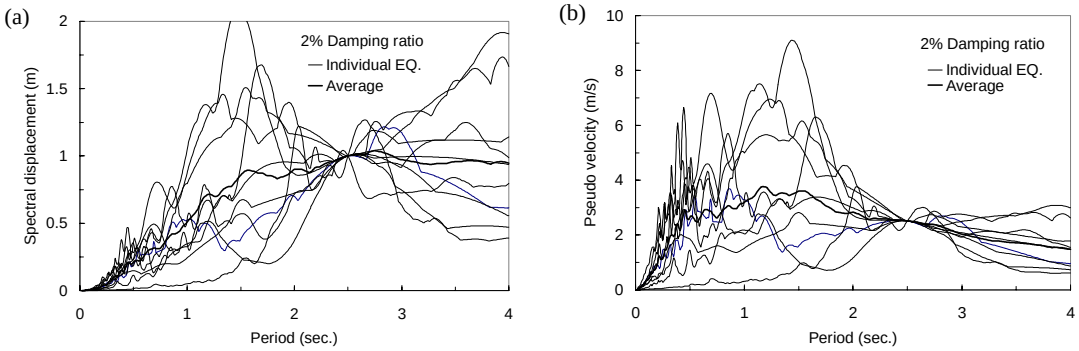

Figure 3. Earthquake spectra: (a) spectral displacement; (b) spectral velocity

Fig. 4 presents typical hysteresis loops obtained for the three damped systems from the dynamic analyses. These loops exhibit the characteristics of the system models described in Figs. 1 and 2. Fig. 5 compares the values of the normalized displacements evaluated from the derived closed-form solution with the corresponding values obtained from dynamic analyses. In the dynamic analyses of the F-PFD and CFD systems, each earthquake record was scaled to five intensity levels, such that the damper slip ratios (μ_s) for these earthquake levels fall within 1 to 40. The normalized displacement function of a T-PFD system does not vary with the earthquake intensity. Hence, this function was verified by changing the value of the T-PFD system parameters, as shown in Fig. 5c and 5d. In general, Fig. 5 illustrates that the proposed closed-form solutions appropriately predict the average normalized displacements for all three systems. Note that the deviation of the response is caused by the diverse frequency contents of the different earthquake records, as evidenced by their spectra (Fig. 3). It is therefore suggested that a sufficient number of earthquake records should be employed when performing dynamic analyses for response investigations.

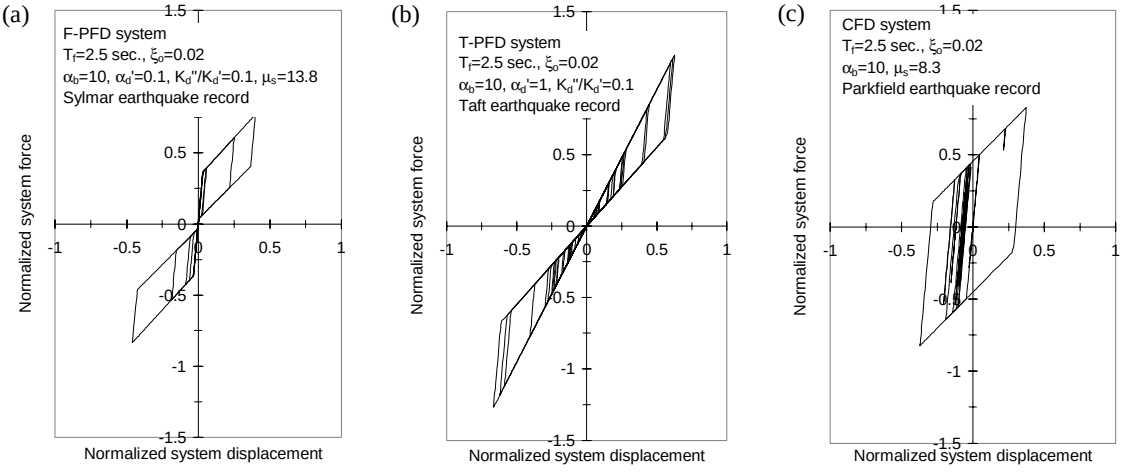

Figure 4. Hysteresis loops resulting from dynamic analyses for: (a) F-PFD; (b) T-PFD; and (c) CFD systems

PARAMETRIC ANALYSIS AND PERFORMANCE COMPARISON

The spectral displacement of a damped system can be evaluated by multiplying the response of the primary system ($S_d(T_f, \xi_o)$) by the normalized displacement function (R_{sd}) corresponding to the selected basic system parameters (α_b, α_d', μ_s, and K_d''/K_d'). Thus, R_{sd} is a measure of the effectiveness of the damper in reducing the seismic response on the basis of a given primary system. In addition to displacement reduction, the system force variation is also an important issue to be considered, since it specifies the system strength requirement. In order

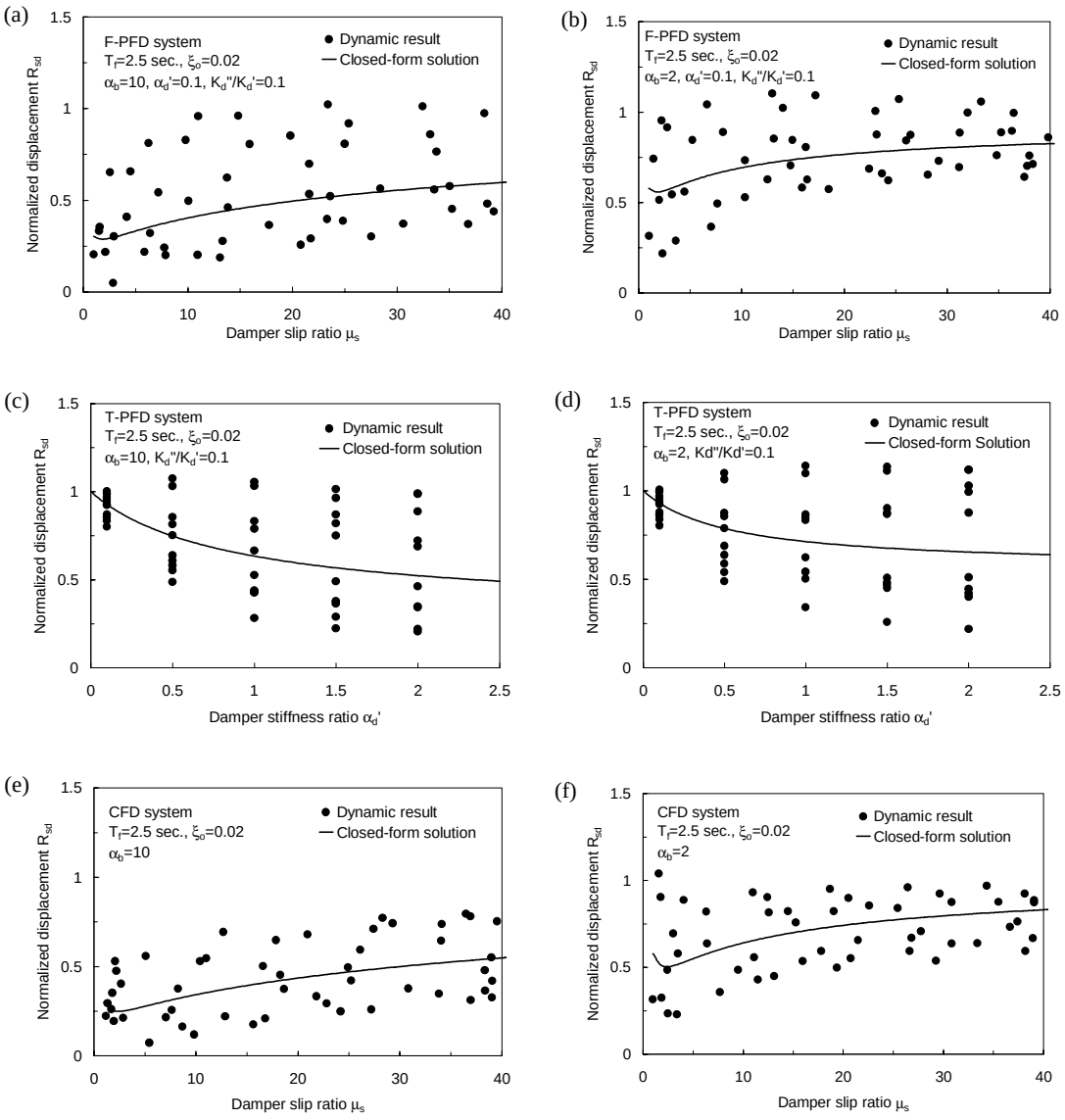

Figure 5. Dynamic verification for normalized displacement: (a) F-PFD system with stiff brace; (b) F-PFD system with soft brace; (c) T-PFD system with stiff brace; (d) T-PFD system with soft brace; (e) CFD system with stiff brace; (f) CFD system with soft brace

to measure the change in system force due to the insertion of a damper into the primary system, a normalized force function, R_f, is defined as the ratio of the damped system force to the primary system force [Fu and Cherry 1999c]. Based on the force-displacement relationships shown in Figs. 1c and 2, the R_f for the F-PFD, T-PFD and CFD systems are, respectively, as follows:

$$R_f = \left[1 + \frac{\alpha_b \alpha_d'}{\alpha_b + \alpha_d'}\left(1 + \frac{\alpha_b}{\alpha_d'}\frac{1}{\mu_s}\right)\right] R_{sd} \qquad (F - PFD\ system) \tag{6a}$$

$$R_f = \left[1 + \frac{\alpha_b \alpha_d'}{\alpha_b + \alpha_d'}\right] R_{sd} \qquad (T - PFD\ system) \tag{6b}$$

$$R_f = \left[1 + \frac{\alpha_b}{\mu_s}\right] R_{sd} \qquad (CFD\ system) \tag{6c}$$

For every set of α_b, α_d', μ_s, K_d''/K_d', there is a pair of R_{sd} and R_f that reflect the damped system performance. From a study of Eqs. 4 and 6, it can be shown that for the F-PFD system, the smaller the α_d', the smaller the R_{sd} and R_f. However, changes in α_d' in the region around α_d'=0.1 result in only slight changes in R_{sd} and R_f. Thus, α_d'=0.1 was selected for the F-PFD parametric analysis. The influence of the variation of K_d''/K_d' on changes in R_{sd} and R_f has a similar effect; changes in K_d''/K_d' in the region around K_d''/K_d'=0.1 result in only slight changes in R_{sd} and R_f. Thus, K_d''/K_d'=0.1 was selected for the PFD parametric analysis.

The variation of R_{sd} and R_f with the basic system parameters are plotted in Fig. 6 for the three described systems. It can be seen that α_b largely determines the ability of the damped system to reduce displacement. The stiffer the brace (larger α_b), the smaller the displacement response. μ_s dominates the force reduction for the F-PFD and CFD systems. As shown in Figs. 6a and 6c, for any given α_b there is an optimal value of μ_s which leads to both small displacement and force response. Essentially, the T-PFD system is a special case of the F-PFD system; it is a F-PFD system whose damper slip ratio μ_s is infinity. In Fig. 6a, the response of the corresponding T-PFD system is located at the extreme right end of the curves. From Fig. 6b, it can be seen that T-PFD systems can also reduce the displacement when α_d' increases, but at the cost of increasing the system force.

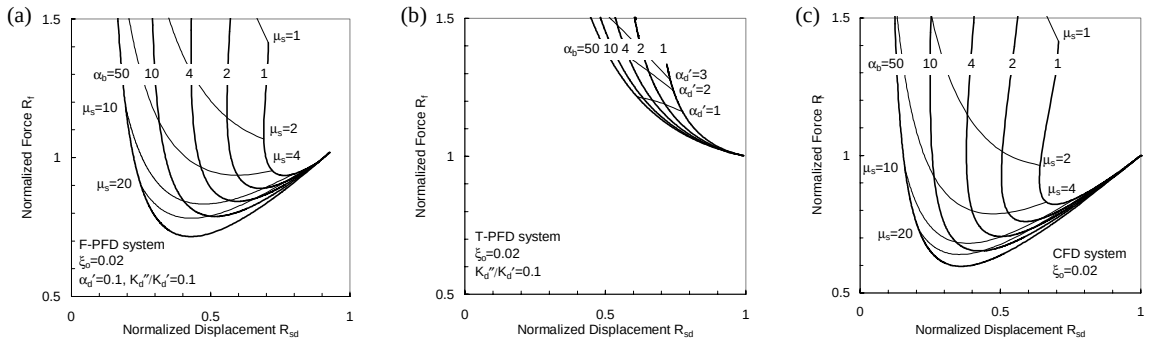

Figure 6. Normalized response: (a) F-PFD system; (b) T-PFD system; (c) CFD system

Figs. 6(a) and 6(c) indicate that that both F-PFD and CFD systems can achieve satisfactory response reduction. When both systems have the same brace stiffness, the CFD system can be expected to exhibit slightly better performance than the F-PFD system. However, due to the large response variation resulting from the stochastic nature of the earthquakes, this superiority may not be realized. Further, it should be noted that, unlike the constant friction damped system, the proportional friction damped system exhibits a self-centering feature that may reduce the cost of any needed repair work after a severe earthquake. The improved performance of the CFD system relative to the F-PFD system results from the fact that its energy dissipation capacity, as defined by hysteresis area, is larger. This, in turn, leads to an increased equivalent damping ratio of the CFD system. At the same time, its equivalent stiffness is similar to the equivalent stiffness of a corresponding F-PFD system. For optimal design of a F-PFD system, parameter values of α_b=4 to 10, μ_s=6 to 15, α_d'=0.1, and K_d''/K_d'=0.1 can be selected to achieve a displacement reduction of about 0.51 to 0.46 and a force reduction of 0.89 to 0.8, relative to the response of its primary system. For optimal design of a CFD system, parameter values of α_b=4 to 10 and μ_s=6 to 12 can be selected to achieve a displacement reduction of about 0.44 to 0.36 and a force reduction of 0.73 to 0.67, relative to the response of its primary system.

In contrast to the F-PFD and CFD systems, the introduction of a T-PFD into a primary system will lead to an increase in system force, although the system displacement may be reduced to some extent. Therefore, it is not recommended that T-PFDs be used to improve the seismic performance of a primary system, unless the resulting force requirement imposed is not a critical issue.

CONCLUSIONS

Closed-form solutions have been derived for the response estimates of proportional friction damped systems. The derived solutions are sufficiently accurate to provide a reasonable estimate of the average spectral response of such systems. These solutions offer a clear indication of the effectiveness of the damper to reduce system response, and can be used to guide the designer to achieve the optimal or desired outcome by appropriate choice of system parameters. The closed-form solutions for proportional friction damped SDOF systems can also be

used to develop procedures for new building design and existing building retrofit of multi-degree of freedom systems, by applying the approach proposed by the authors in their treatment of constant friction damped systems, [Fu and Cherry 1999c, 1998] and [Fu and Cherry 1999a, 1999b], respectively.

Proportional friction damped systems exhibiting triangular hysteresis loops are not capable of reducing the system force; they are therefore not recommended for application in normal situations. Due to its greater energy dissipation capacity, the response reduction associated with constant friction damped systems is expected to be larger than the response reduction of proportional friction damped systems. However, because of the stochastic nature of earthquakes, the response difference between these two systems may be negligible.

REFERENCES

Aiken, I.D. and Kelly, J.M. (1990), *Earthquake Simulator Testing and Analysis Studies of Two Energy-Absorbing Systems for Multistorey Structures*, Report No. UCB/EERC-90/03, Earthquake Engineering Research Center, University of California at Berkeley, California, USA.

Carr, A.J. (1998), *RUAUMOKO – The Maori God of Volcanoes and Earthquake*, Computer Program Library, Department of Civil Engineering, University of Canterbury, New Zealand.

Filiatrault, A. and Cherry, S. (1987), "Experimental studies of friction damped braced steel frames", *5th Canadian Conference on Earthquake Engineering*, Ottawa, Canada, July 6-8, pp867-873.

Fu, Y. (1996), "Frame retrofit by using viscous and viscoelastic dampers", *Proceedings of Eleventh World Conference on Earthquake Engineering*, Paper No. 428.

Fu, Y. and Cherry, S. (1998), "Quasi-static design procedure for friction damped structures", *Proceedings of Second World Conference on Structural Control*, Kyoto, Japan, June 28 - July 2, 93-102.

Fu, Y. and Cherry, S. (1999a), "Frame retrofit using friction dampers", *Proceedings of 8th Canadian Conference on Earthquake Engineering*, Vancouver, Canada, June, pp385-390.

Fu, Y. and Cherry, S. (1999b), "Quasi-static retrofit analysis for friction damped frames", Presented at *International Workshop on Seismic Isolation, Energy Dissipation and Control of Structures*, Guangzhou, China, May.

Fu, Y. and Cherry, S. (1999c), "Simplified seismic code design procedure for friction damped steel frames", *Canadian Journal of Civil Engineering*, 26, pp55-71.

Fu, Y. and Kasai, K. (1998), "Comparative study of frames using viscoelastic and viscous dampers", *ASCE, Journal of Structural Engineering*, 124, pp513-522.

Grigorian, C.E. and Popov, E.P. (1993), "Slotted bolted connections for energy dissipation", *Proceedings of the ATC-17-1 Seminar on Seismic Isolation, Passive Energy Dissipation, and Active Control*, San Francisco, California, USA, pp545-556.

Hanson, R.D. and Jeong, S.M. (1994), "Design procedure utilizing supplemental energy dissipation devices for improved building performance", *Proceedings of fifth U.S. National Conference on Earthquake Engineering*, pp517-526.

Iwan, W.D. and Gates, N.C. (1979), "Estimating earthquake response of simple hysteretic structures", *ASCE, Journal of Engineering Mechanics*, Division, EM3: pp391-405.

Kar, R., Rainer, J.H. and Lefrancois, A.C. (1996), "Dynamic properties of a circuit breaker with friction based seismic dampers", *Earthquake Spectra*, 12, 2, pp297-314.

Kasai, K., Fu, Y. and Watanabe, A. (1998), "Two types of passive control systems for seismic damage mitigation", *ASCE, Journal of Structural Engineering*, 124, pp501-512.

Nims, D.K., Richter, P.J. and Bachman, R.E. (1993), "The use of the energy dissipating restraint for seismic hazard mitigation", *Earthquake Spectra*, 9, 3, pp467-489.

Pall, A.S. and Marsh, C. (1982), "Response of friction damped braced frame", *ASCE, Journal of Structural Division*, 108(ST6): pp1313-1323.

Shepherd, R., and Erasmus, L.A. (1988), "Ring spring energy dissipators in seismic resistant structures", *9th World Conference on Earthquake Engineering*, Japan, 5, pp767-772.

Tremblay, R. and Stiemer, S.F. (1993), "Energy dissipation through friction bolted connections in concentrically braced steel frames" *Proceedings of the ATC-17-1 Seminar on Seismic Isolation, Passive Energy Dissipation, and Active Control*, San Francisco, California, USA, pp. 557-568.

Watanabe, A. (1996), "Some damage control criteria for steel building with added hysteresis damper", *Proceedings of Eleventh World Conference on Earthquake*, Paper No. 449.